IEEE Access
Multidisciplinary | Rapid Review | Open Access Journal

Received April 11, 2019, accepted May 8, 2019, date of publication May 20, 2019, date of current version June 13, 2019.

Digital Object Identifier 10.1109/ACCESS.2019.2918029

Health Condition Assessment of Base-Plate Solder for Multi-Chip IGBT Module in Wind Power Converter

YAOGANG HU[1,3], PINGPING SHI[2], HUI LI[4], AND CHAO YANG[1,3]

[1]School of Electrical and Electronic Engineering, Chongqing University of Technology, Chongqing 400054, China
[2]School of Management, Chongqing University of Technology, Chongqing 400054, China
[3]Energy Internet Engineering Technology Center of Chongqing City, Chongqing 400054, China
[4]State Key Laboratory of Equipment and System Safety of Power Transmission and Distribution and New Technology, Chongqing University, Chongqing 400044, China

Corresponding authors: Pingping Shi (spprabbit@163.com) and Chao Yang (esyangchao@163.com)

This work was supported in part by the National Natural Science Foundation of China under Grant 51675354, in part by the International Cooperation and Exchange Projects in NSFC under Grant 51761135014, in part by the Fundamental Research Funds for the Central Universities under Grant 106112017CDJZRPY0007, in part by the Chongqing Artificial Intelligence Technology Innovation Project under Grant cstc2017rgzn-zdyf0117, and in part by the Scientific Research Foundation of Chongqing University of Technology.

ABSTRACT The base-plate solder fatigue of the IGBT module is one of the failures of the wind power converter; however, the existing health condition monitoring method based on infrared thermography is difficult to be applied to the actual applications. In this paper, a health condition assessment method of the base-plate solder fatigue for the IGBT module is introduced based on the case temperature difference. First, according to the structure of the IGBT module, a 3D finite element model is established, and the junction and case temperatures at different delamination degrees are investigated. Second, for defining the degradation degree, identifying the steady-state process, and acquiring the case temperature, an assessment method of the base-plate solder fatigue based on the case temperature difference is established. Finally, taking the experiment of a practical wind turbine converter IGBT module as an example, the assessment process of base-plate solder of the IGBT module is demonstrated, and the results show that the proposed assessment method is correct and effective.

INDEX TERMS Wind power converters, multi-chip IGBT module, base-plate solder, health condition monitoring.

I. INTRODUCTION

The IGBT module is the essential part of wind power converter [1]–[3]. However, failure rate of IGBT module, which reaches more than 30% [4], [5], is much higher than other parts [6]. Because wind turbines suffer long-term, frequent and wide range of random output changes, energy conversion unit continues to afford severe thermal stress impacts [7]–[9], and the alternating thermal impacts generated between the layers of IGBT module will cause fatigue cracks in the solder layer and solder off. In order to obtain the health conditions of IGBT module early, it is necessary to study the temperature distribution law and condition evaluation of IGBT module in wind power converter.

The solder layer of IGBT module includes chip solder layer and base-plate solder layer. Compare with the chip solder, the base-plate solder delamination can change the temperature distribution of entire IGBT module, moreover, the lifetime and reliability of IGBT module are seriously influenced. Currently, the solder delamination study of IGBT module is in the initial stage, and its temperature distribution and monitoring methods are mainly focused. In the research aspect of temperature distribution of IGBT module, In [10], [11], the relationship between delamination degree of base-plate solder and corresponding temperature are obtained by establishing a 3D finite element model of IGBT module, and the results indicate that the failure possibility of IGBT module will increase when the delamination degree is greater than 50% [11]. In literature [12], the failure behavior of solder joint is discussed; the effects of voids on the thermal-mechanical characteristic are analyzed. Results indicate the max value of thermal stress locates on the edge of solder layer and the martin of void, and the junction temperature increases exponentially with the radius of the void. In terms

The associate editor coordinating the review of this manuscript and approving it for publication was Ramani Kannan.

of condition monitoring research, the literature [12] proposed a method based on temperature gradient for evaluating the operation conditions of solder layer, however, considering that the actual IGBT modules are generally placed into the converter, it is difficult to obtain the surface junction temperature gradient through the infrared monitoring equipment, which is more difficult in practical application. The IGBT module bears different varieties of thermal stress fatigue load, therefore, the health condition is gradually deteriorating in the course of long-term operation. When the phenomenon of base-plate solder delamination appears, the internal physical structure of IGBT module is changed, and the IGBT module junction temperature and case temperature are further increased [13], [14], which change the chip case temperature and the degree of thermal coupling among the chips. In literature [15], based on the case temperature, the thermal resistances are calculated by using the power loss model, and a condition monitoring method of single-chip IGBT device is proposed by using changed thermal resistance. However, the multi-chip IGBT module, due to the difference in the spatial position of the chip and the thermal coupling between the chips, is difficult to calculate the junction temperature accurately by the loss model, furthermore, it is difficult to obtain the thermal resistance changes. Therefore, it is necessary to study the characteristics of base-plate solder delamination, and health condition assessment method of base-plate solder for multi-chip IGBT module in wind power converter should be proposed and be easy to use.

The contributions of this paper include presenting a health condition assessment method of base-plate solder for multi-chip IGBT module in wind power converter based on case temperature difference. In Section II, according to material characteristics parameters of an actual wind power converter IGBT module, a 3D finite element model of IGBT module is established. In Section III, the changes of junction temperature and case temperature of IGBT module under different delamination degrees are studied. In Section V, a health condition assessment method of base-plate solder for multi-chip IGBT module is proposed. In Section VI, a case is investigated to validate the proposed method. In Section VII, the conclusion is presented.

II. IGBT MODULE OF WIND POWER CONVERTER AND ITS FINITE ELEMENT MODELING

A. IGBT MODULE STRUCTURE OF WIND POWER CONVERTER

In this paper, an IGBT module of 1.5 MW WTGS wind power converter (ID: Infineon FF450R17ME4) is as the object to research. The rotor-side converter (RSC) of wind power converter, as shown in Figure 1(a), consists of two groups of three-phase full-bridge circuit in parallel. Figure 1(b) shows that each phase upper and lower bridge leg includes an IGBT module and its drive circuit board. The module contains six IGBT chips, which is shown in Figure 2(a). Each IGBT chip is connected in parallel with a Free-Wheeling Diode (FWD) chip, connecting via the aluminum bonding wires as well.

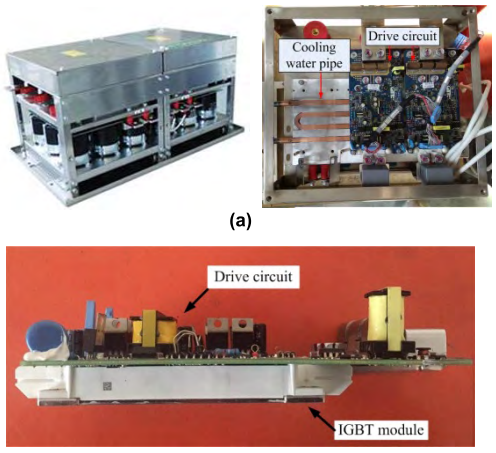

FIGURE 1. Wind power converter and its IGBT module. (a) Machine-side converter and its internal structure. (b) IGBT module and its drive circuit board.

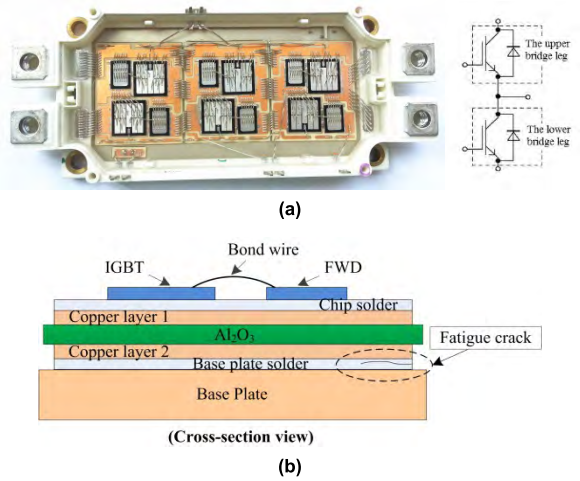

FIGURE 2. IGBT module and its cross-section view. (a) IGBT module and its internal equivalent circuit. (b) Cross-section view of the IGBT module.

The IGBT chips of upper and lower bridge leg are placed in series, and the IGBT module is on a water cooled radiator. In addition, Figure 2(b) shows that the structure of the layer of the IGBT module includes seven layers. Both the copper and ceramic layers comprise the direct bonded copper layer, which is connected to the base-plate by the solder. Each layer of the IGBT module has different coefficients of thermal expansion (CTE), which result in the occurrence of alternating thermal stress between the two layers with temperature changes [11]–[13]. This kind of CTE mismatch causes fatigue cracks, which affect the heat dissipation of the IGBT chips. The concentration of extra temperature and the severe mechanical deformations enlarge the area of fatigue cracks and cause the desquamating part of the base-plate solder.

B. FINITE ELEMENT MODELING OF IGBT MODULE

The finite element modeling is divided into three steps: building the geometric model of IGBT module, assigning the

TABLE 1. Geometrical parameters of IGBT module.

IGBT module	Material	Resistivity /Ω•m	Temperature coefficient of resistance	Size /mm	Thermal Conductivity /W•(m•K)$^{-1}$	Poisson's ratio	Young's modulus /MPa
Bond wire	Al	$2.85*10^{-8}$	0.0037	radius:0.15	238	0.33	70000
IGBT	Si	/	/	13×13×0.5	139	0.28	112000
Solder 1	Sn-Ag-Cu	$3.56*10^{-7}$	0.0024	33×38×0.1	78	0.4	43000
Copper layer 1	Cu	$1.72*10^{-8}$	0.0039	33×38×0.2	386	0.34	110000
Ceramic	Al_2O_3	$1*10^{22}$	0	100×40×0.4	18	0.22	370000
Copper layer 2	Cu	$1.72*10^{-8}$	0.0039	100×40×0.2	386	0.34	110000
Solder 2	Sn-Ag-Cu	$3.56*10^{-7}$	0.0024	100×40×0.1	78	0.4	43000
Base Plate	Cu	$1.72*10^{-8}$	0.0039	122×62×3	386	0.34	110000

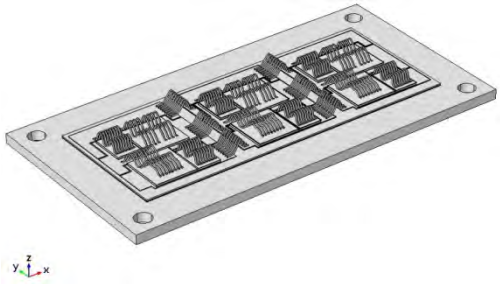

FIGURE 3. 3D finite element model of IGBT module.

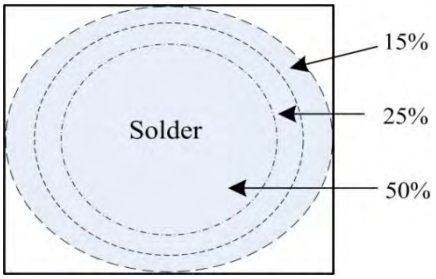

FIGURE 4. Desquamating degree of solder delamination.

TABLE 2. Equivalent resistance and its resistance coefficient of IGBT chips.

Conduction current /A	30	60	90	120	150
Resistance /Ω	0.104	0.0575	0.041	0.0328	0.028
Voltage /V	1.04	1.15	1.23	1.312	1.4
Temperature coefficient	-0.00405	-0.00061	0	0.00031	0.00036
Conduction current /A	180	210	240	270	300
Resistance /Ω	0.0242	0.022	0.02	0.0183	0.0173
Voltage /V	1.452	1.54	1.6	1.647	1.73
Temperature coefficient	0.00089	0.00084	0.00119	0.00139	0.00139

material property and setting the electro thermal coupling physical field boundary condition [16].

(1) Building the geometric model of IGBT module. According to the structure and size of the IGBT module (Table 1[17]), the geometric model of IGBT module is established using the geometrical design tool of COMSOL Multiphysics, and the established 3D finite element model is in Figure 3.

(2) Assigning the material property. According to the material parameters of the IGBT module in Table 1, the material values of the constructed finite element model are assigned. Especially, because the equivalent resistance value of silicon is affected easily by the temperature, the equivalent attribute values of silicon are assigned based on the IGBT module technical information in Table 2.

(3) Setting the physical field boundary condition. Considering the operational characteristics of IGBT module is affected mainly by electro-thermal coupling physical fields, in the boundary condition aspect, the IGBT chips, copper layer near chips and bonding wire as the heat sources are assigned. Besides, the heat dissipation of IGBT module is only through the bottom cooling surface, and the ambient temperature is set to 20° C.

III. THERMAL ANALYSIS OF IGBT MODULE UNDER THE BASE-PLATE SOLDER DELAMINATION

A. TEMPERATURE DISTRIBUTION OF IGBT MODULE UNDER THE BASE-PLATE SOLDER DELAMINATION

Because the IGBT chip's conduction voltage and conduction loss are relatively larger than the FWD chip's, in this section the FWD may be neglected, and the IGBT chips of upper bridge leg inside IGBT module as the research object may be selected. In order to reduce the simulation time, the bonding wires of FWD chips and IGBT chips of lower arm are removed in Figure 3, before the finite element simulation is carried out. Furthermore, In order to grasp the temperature distribution of the IGBT module, the concept of desquamating degree is introduced to characterize the degree of solder delamination [13], which is the proportion of the remaining area to the total area of solder layer, and the different desquamating degrees are shown in Figure 4. When the desquamating degree of base-plate solder layer is 0%, 8%, 17%, 34%, respectively, the conditions of base-plate solder delamination are shown in Figure 5.

When the conduction current is 50A, the junction temperature distribution of IGBT module under different

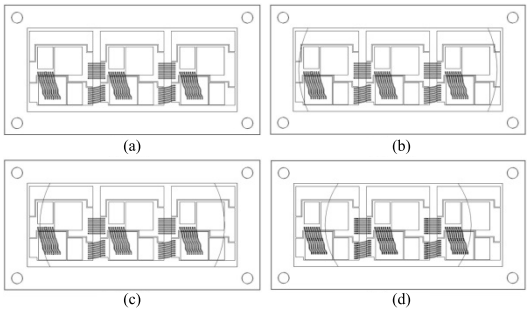

FIGURE 5. Condition of base-plate solder delamination of IGBT module. (a) 0%. (b) 8%. (c) 17%. (d) 34%.

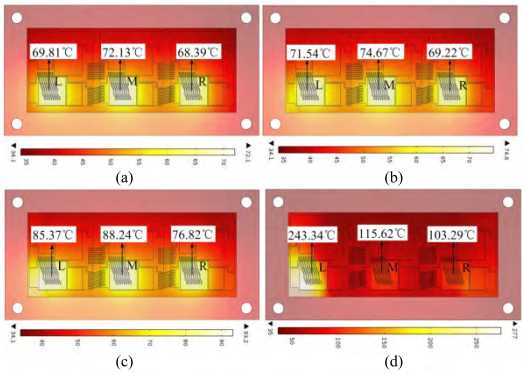

FIGURE 6. Temperature distribution of IGBT module under different desquamating degrees. (a) 0%. (b) 8%. (c) 17%. (d) 34%.

desquamating degrees is shown in Figure 6 by the finite element simulation. When the desquamating degree is 8%, compared with no damage condition in Figure 6(a), the junction temperature of IGBT chips has no significant change, just the junction temperature of chip M is slightly higher than the chip on both sides 3∼4° C. Moreover, when the shedding degree is 17% and 34%, the junction temperature has a significant increase. Since the position of chip L is close to the left edge of the IGBT module, compared with chip R, the junction temperature of chip L change is more obvious, when the shedding area of left and right side layer is same. Since the base-plate solder under the chip L is almost entirely shed off when the desquamating degree is 34%, the heat transfer path has changed dramatically, and the junction temperature of chip L rises to 243.34° C.

In addition, when the desquamating degree is 0%, 8%, 17%, 34%, the case temperature distribution of the IGBT module is shown in Figure 7. Compared with no damage condition in Figure 7(a), the maximum case temperature change of each chip is not obvious, the case temperature of chip M rises by only 0.45° C. Because solder delamination gradually results in the increase of thermal resistance, the concentrated heat have to be dissipated in the central part of IGBT module through the remaining non-shedding base-plate solder. When the shedding degree is 17% and 34%, the highest case temperature of each chip has increased differently, and the junction temperature of chip M increase by 10.7° C and 32.41° C respectively.

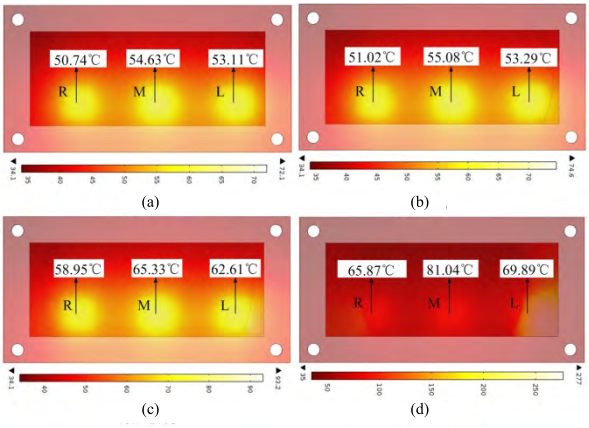

FIGURE 7. Case temperature distribution of IGBT module under different desquamating degrees. (a) 0%. (b) 8%. (c) 17%. (d) 34%.

B. ANALYSIS OF TEMPERATURE DIFFERENCE AMONG IGBT CHIPS

When the junction temperature change of IGBT chip with time around a temperature value fluctuates regularly, the IGBT chip can be considered that the temperature is in the steady state stage. The RSC generally is controlled by the SVPWM strategy [18], and the conduction time of phase current through the IGBT chip account for 1/2 cycle. When the effective value of phase current is 50A, the frequency of phase current is 5Hz and the initial junction temperature of IGBT ship is 20° C,by the finite element simulation the junction temperature and case temperature are shown in Figure 8(a). After transient process about 15s, the junction temperature and case temperature turn into the steady state stage; their fluctuation process is shown in Figure 8(b), and the junction temperature and case temperature of chip M are higher than other chips. In addition, compared with the temperature fluctuation of junction temperature, case temperature fluctuations are smaller. Besides, the stability of temperature difference, as shown in Figure 8(c), is basically similar, the temperature difference T_{ML} between chip M and chip L is about 1.5° C, and T_{MR} is about 3.9° C. In summary, no matter how fluctuate the case temperatures, the steady-state case temperature remains relatively constant. Therefore, it is possible to consider the steady-state temperature difference as an effective characteristic quantity for reflecting the heath condition of base-plate solder.

IV. ASSESSMENT METHOD OF BASE-PLATE SOLDER OF IGBT MODULE

A. ASSESSMENT MODEL OF BASE-PLATE SOLDER OF IGBT MODULE

(1) Chip positioning

Considering that the early solder delamination occurs first at the four corners of the IGBT module, all IGBT ships should be named respectively. In Figure 6 the two IGBT chips are called chip L and chip R, which are closest to the left and right sides of the IGBT module. In addition, the chip, called chip M, is selected from the center IGBT chip in the IGBT

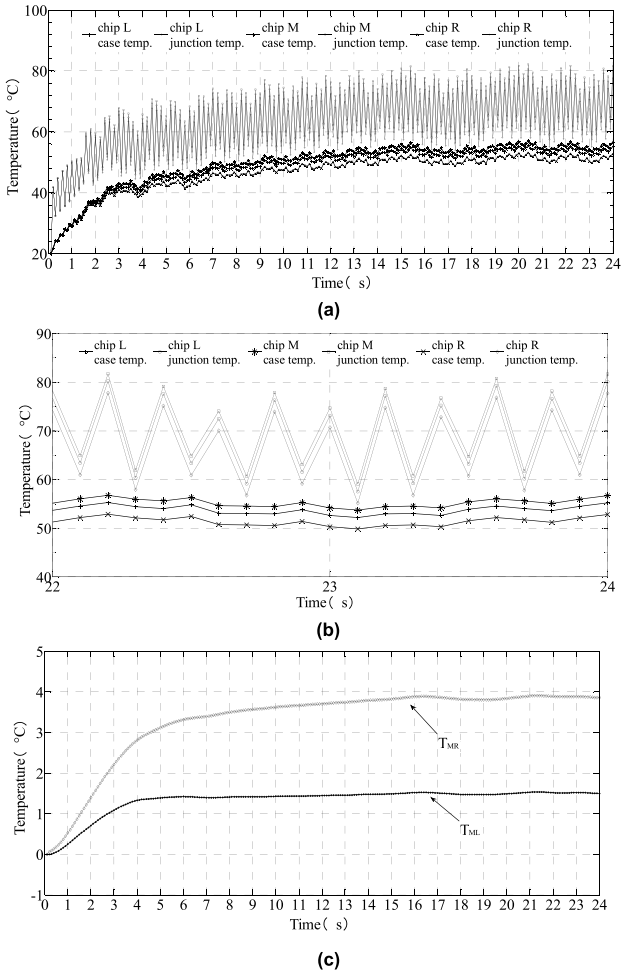

FIGURE 8. Change condition of junction temperature and case temperature of IGBT chips. (a) Temperature change trend. (b) Steady state stage. (c) Chip shell temperature difference.

module as far as possible, and the case temperature of chip L, R, M are denoted by T_{L}, T_{M} and T_{R}.

(2) Acquiring steady state case temperature of IGBT chip

The change of operation condition will cause the internal temperature distribution of IGBT module to change. In order to obtain the steady state case temperature, the processes is made and introduced as follows.

Firstly, extracting case temperature time series data $(T_{\mathrm{L}}^{(0)}, T_{\mathrm{M}}^{(0)}, T_{\mathrm{R}}^{(0)})$, $(T_{\mathrm{L}}^{(1)}, T_{\mathrm{M}}^{(1)}, T_{\mathrm{R}}^{(1)}), \ldots, (T_{\mathrm{L}}^{(n)}, T_{\mathrm{M}}^{(n)}, T_{\mathrm{R}}^{(n)})$. Secondly, acquiring the case temperature difference $(T_{\mathrm{ML}}^{(0)}, T_{\mathrm{MR}}^{(0)})$, $(T_{\mathrm{ML}}^{(1)}, T_{\mathrm{MR}}^{(1)}), \ldots, (T_{\mathrm{ML}}^{(n)}, T_{\mathrm{MR}}^{(n)})$, where, $T_{\mathrm{M}i} = T_{\mathrm{M}}$-$T_i$, $(i = \mathrm{L}, \mathrm{R})$. Thirdly, finding the increment of case temperature difference $(\Delta T_{\mathrm{ML}}^{(1)}, \Delta T_{\mathrm{MR}}^{(1)})$, $(\Delta T_{\mathrm{ML}}^{(2)}, \Delta T_{\mathrm{MR}}^{(2)}), \ldots, (\Delta T_{\mathrm{ML}}^{(n)}, \Delta T_{\mathrm{MR}}^{(n)})$, where the formula of $\Delta T_{\mathrm{M}i}^{(n)}$ is

$$\Delta T_{\mathrm{M}i}^{(n)} = T_{\mathrm{M}i}^{(n)} - T_{\mathrm{M}i}^{(n-1)}, \quad (i = \mathrm{L}, \mathrm{R}) \tag{1}$$

Finally, when $\Delta T_{\mathrm{ML}}^{(j)} = \Delta T_{\mathrm{MR}}^{(j)} = 0$, steady state case temperature are $T_{\mathrm{L}}^{(j)}$, $T_{\mathrm{M}}^{(j)}$ and $T_{\mathrm{R}}^{(j)}$ respectively.

(3) Determination processes of normal case temperature based on BP neural network.

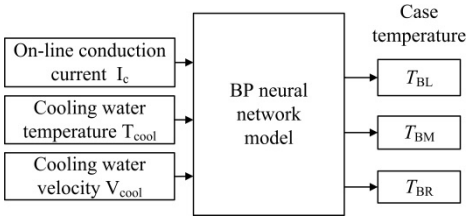

FIGURE 9. Input and output of BP neutral networks.

In order to obtain the normal case temperature values under different operation conditions, a 3-layer BP neural network model of 3-input and 3-output is established (Figure 9). The input parameters are the conduction current $\mathrm{I_c}$, the cooling water temperature $\mathrm{T_{cool}}$, and the cooling water flow rate $\mathrm{V_{cool}}$, and the output parameters are T_{BL}, T_{BM} and T_{BR}. The case temperature data of new IGBT module may be generally considered as the normal data, and these normal case temperature data are used as training samples of BP neural network.

(4) Degradation degree for base-plate solder

With the base-plate solder shedding off, the junction temperature of the chips L, R, M will rise to varying degrees. In general, the left and right side of the solder will appear different shedding degrees. The more the shedding area is, the higher the case temperature is. Therefore, compared to judge by both monitored two sides case temperature and its normal case temperature, the maximum temperature difference can represent the deterioration condition of the base-plate solder. In order to quantify the degradation of base-plate solder, the concept of deterioration degree is used, and the temperature difference between the chips is adopted to reflect the base-plate solder degradation. The formula of deterioration degree g is,

$$g(T_{\mathrm{M}i}) = \frac{T_{\mathrm{M}i} - T_{\mathrm{BM}i}}{T_{\mathrm{BM}i}}, \tag{2}$$

where, $T_{\mathrm{BM}i} = T_{\mathrm{BM}}$-$T_{\mathrm{B}i}$, $(i = \mathrm{L}, \mathrm{R})$. Based on Classification of wind turbine assessment indicators in literature [19], the deterioration degree is divided into four grades: $L = \{l_1, l_2, l_3, l_4\}$ = {Excellent, Good, Alert, Danger}. The deterioration degree is defined as follows: $l_1 \in [0,0.30]$, $l_2 \in [0.30,0.55]$, $l_3 \in [0.55,0.80]$, $l_4 \in [0.80,\infty]$.

B. EVALUATION PROCEDURE OF BASE-PLATE SOLDER OF IGBT MODULE

Based on the case temperature time series data of the IGBT chips L, R, and M, after determining the steady-state case temperature, the deterioration degree is obtained according to calculation flowchart of degradation degree in Figure 10. Firstly, the on-line conduction current $\mathrm{I_c}$, the cooling water temperature T_{cool}, and the cooling water flow rate $\mathrm{V_{cool}}$ are as the input of BP neural network model. Secondly, determine the measured case temperature of the left and right sides of IGBT ship and their temperature difference based on the normal case temperature. Thirdly, If T_{LL} is greater than T_{RR}, the left side of desquamating degree is larger. According

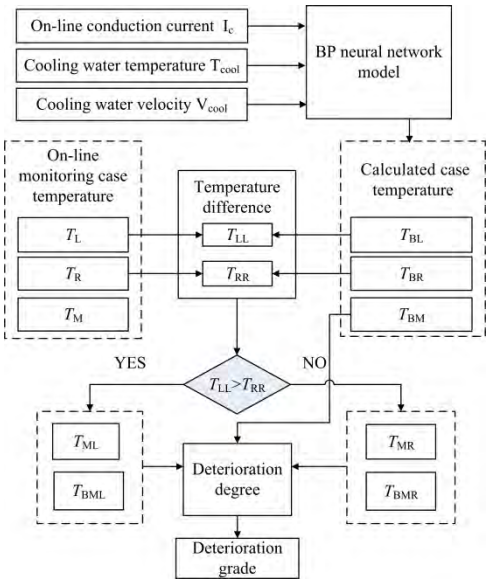

FIGURE 10. Assessment flowchart of degradation degree for base-plate solder of IGBT module.

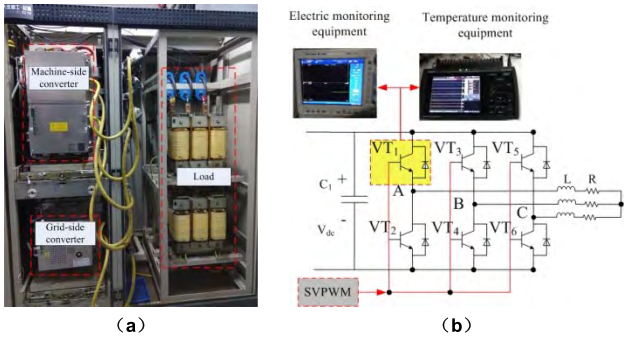

(a) (b)

FIGURE 11. Experiment platform of wind power converter and schematic of the equivalent experiment setup. (a) Experiment platform. (b) Experimental structure of RSC.

to the measured temperature difference between the left and the normal temperature difference, the degradation degree is calculated by the formula (2). On contrary, through the right side of the measured temperature difference and the normal temperature difference, the degradation degree is calculated by the formula (2).

V. EXPERIMENT VERIFICATION

A. INTRODUCTION OF THE EXPERIMENT PLATFORM

In order to verify the validity of the established finite element model and the proposed evaluation method, according to experiment in [13], using the wind turbine converter platform from a converter company, adding a 1 mm thick metal plate under the bottom of IGBT module, installing the temperature sensor at the bottom of each IGBT chip, the shedding process of base-plate solder is simulated by changing the area of the metal plate. The smaller the area of the metal plate is, the greater the desquamating degree is.

The experimental platform and its electrical structure are shown in Figure 11, which mainly include a RSC, a gird side converter, a cooling device, an inductive load. The control

TABLE 3. Parameters of experiment equipment.

Monitoring equipment and parameters	Equipment type and parameter values
DC voltage V_{dc}	1050 V
Capacitor C_1	2350 F
Switch frequency f_s	3000Hz
Resistance R	0.01Ω
Inductance L	0.4mH
Temperature monitoring equipment	OMRON ZR-RX45
Electric monitoring equipment	YOKOGAWA DL850

FIGURE 12. Experiment of IGBT module under the health base-plate solder.

system of wind power converter can adjust the cooling water flow rate, amplitude and frequency of phase current, and monitor the cooling water temperature and other parameters. The DC power supply V_{dc} is provided through the gird side converter and DC link, and the resistor and inductor is as the circuit load. Using the open-loop control with SVPWM strategy, the experimental IGBT module turns on and off orderly. The IGBT module VT_1 is taken as the experiment object, the conduction current and the case temperature of each chip of VT_1 are collected by the current and temperature monitoring equipment, and the monitoring parameters and acquisition equipment are shown in Table 3.

B. VALIDATION OF FINITE ELEMENT MODEL VALIDITY

In this section, the validity of established finite element model is proved by the comparison between the calculated and monitoring case temperature, when the base-plate solder is no damage. In Figure 12, three temperature sensors are fixed at the bottom of tested IGBT module by the slotted metal plate, and the tested IGBT module and the slotted metal plate are installed together with heat-conducting glue. In addition, the IGBT module and its drive circuit board placed on the cooling device, as shown in Figure 1(b). When the RSC current is set to 30A, 50A and 75A respectively, the monitored case temperature are shown in Figure 13.

Figure 13 indicates that when the IGBT module is turned on, as in Figure 8, the case temperature rises to steady state after a brief transient process (about 60s). In addition, the steady-state case temperatures of each chip rise with the increase of current gradually. Comparing the calculated values of finite element simulation

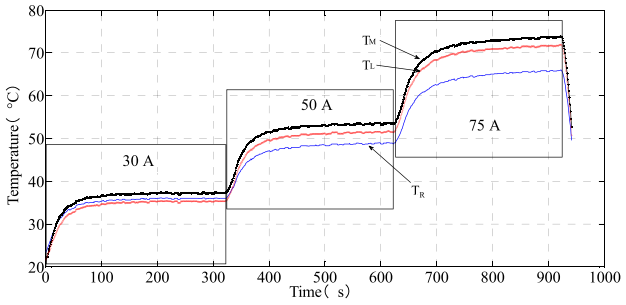

FIGURE 13. Change condition of case temperature at different currents.

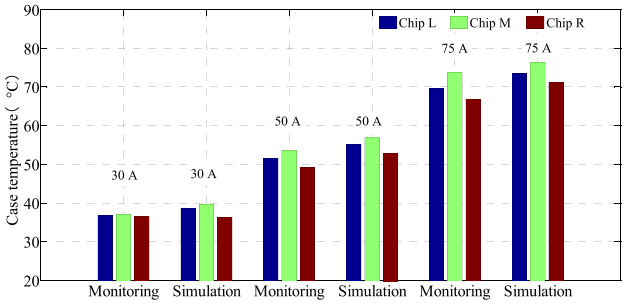

FIGURE 14. Case temperature of IGBT chips at different currents.

TABLE 4. Case temperature difference of IGBT chips at different currents.

Case temperature difference		Current		
		30 A	50 A	75 A
T_{ML}	Monitoring	1.1°C	2.0°C	3.2°C
	Calculation	1.2°C	1.5°C	2.8°C
T_{MR}	Monitoring	1.4°C	4.5°C	6.5°C
	Calculation	3.4°C	3.9°C	5.2°C

in Figure 14 with the monitored in Figure 13, under the same current excitation, the case temperature difference is extremely small.

The steady-state temperature difference of each ship between the simulated and the monitored conditions are in Table 4 under different currents. It can be seen from Table 4 that the relative case temperature difference of each chip is slightly different, the reason is that the simulation values is obtained by the ideal current excitation and heat dissipation conditions. Besides, the actual IGBT module is also affected by many factors, such as, cooling conditions, the measurement accuracy of temperature sensor, and so on.

From the above comparison, the case temperature change trend of both the simulated and monitored is similar, and both kinds of temperature value are almost equal. Therefore, the established 3D finite element model is valid.

C. VALIDITY OF ASSESSMENT METHOD OF BASE-PLATE SOLDER

(1) Sample acquisition and validation of BP neural network

It takes a long time to obtain a large number of experiment samples, therefore, using the established finite element model, the sample training data needed to the BP neural network are obtained. Because the wind power converter for experiment is two parallel structures and its IGBT modules need to reserve a large working margin, which are generally 2-3 times of the maximum conduction current, therefore, the actual conduction current range of each IGBT module should be is 50∼100A.

TABLE 5. Comparison of steady state case temperature by using the actual measurement and BP neural network.

Current		Case temperature		
		Chip L	Chip M	Chip R
30 A	Monitoring values	36.7°C	37.8°C	36.4°C
	Calculation values	36.1°C	38.4°C	35.7°C
	Error	-1.66%	1.56%	-1.96%
50 A	Monitoring values	51.6°C	53.6°C	49.1°C
	Calculation values	50.4°C	54.8°C	49.8°C
	Error	-2.38%	2.19%	1.41%
75 A	Monitoring values	70.7°C	73.9°C	67.4°C
	Calculation values	69.6°C	74.7°C	68.1°C
	Error	-1.58%	1.07%	1.03%

When the desquamating degree is 0%, the currents are 50A, 60A, 70A, 80A, 90A and 100A respectively, the cooling water temperatures are 20° C, 30° C and 40° C respectively, cooling water flow rate are 0.75 m/s, 1 m/s and 1.25 m/s respectively, the finite element simulation is carried out, and the simulation data as training samples are obtained. Comparison of steady state case temperature in Table 5 indicates that the absolute value of maximum error is 2.38%. In addition, the temperature difference between the calculated and the monitored is only 1.2° C. Therefore, the trained BP neural network can meet the accuracy requirements.

(2) Calculation of deterioration degree of base-plate solder fatigue.

In order to verify the validity of the proposed assessment model, the several stages of base-plate solder fatigue are simulated by cutting the four corners of the metal plate. In Figure 15, the left and right sides of metal plate are cut symmetrically, and the cut area account for the original area of 17%, namely, the desquamating degree is 17%.

When the conduction currents are 30A, 50A and 75A respectively, the range of cooling water temperature is 21∼21.5° C, the cooling water flow rate is 1m/s, the changes of monitored case temperature are shown in Figure 16.

Based on the Figure 14, the steady state case temperature of two conditions, which are both desquamating degree 0% and 17%, are listed in Table 6. Compared with the condition of desquamating degree 0%, when desquamating degree is 17%, under different currents, the case temperature increase in different degrees, especially, T_M has the largest increase, which are 4.3° C, 10.0° C and 13.2° C respectively.

Based on the assessment process in section III.B, the calculation steps of deterioration degree are as follows.

FIGURE 15. Metal plate by cutting the 17% area.

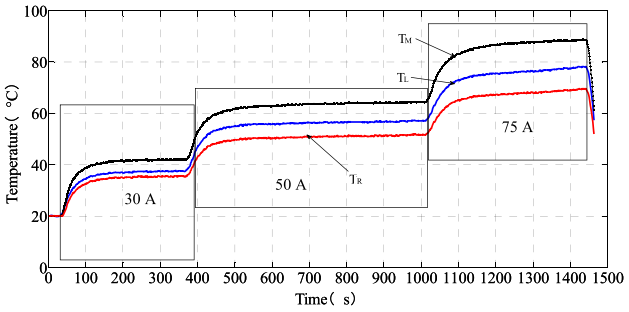

FIGURE 16. Change condition of case temperature of IGBT chips under the metal plate by cutting the 17% area.

TABLE 6. Comparison of steady state case temperature between the desquamating degrees 0% and 17%.

Case temperature	desquamating degrees 0%			desquamating degrees 17%		
	30 A	50 A	75 A	30 A	50 A	75 A
T_L	36.7°C	51.6°C	70.7°C	38.2°C	56.3°C	78.3°C
T_M	37.8°C	53.6°C	73.9°C	42.1°C	63.6°C	87.1°C
T_R	36.4°C	49.1°C	67.4°C	37.6°C	51.4°C	69.8°C

1) Obtaining the steady state case temperature difference of desquamating degree 0%

According to the Table 5, the steady state case temperature of deterioration degree 0% is obtained by the BP neural network, when the current is 30 A, 50 A and 75 A. Moreover, the steady state case temperature difference T_{BML} and T_{BMR} are calculated, as shown in Table 7.

2) Obtaining the steady state case temperature difference under different desquamating degrees

According to the case temperature data in Table 6, the monitored T_{ML} and T_{MR} are obtained under different currents, as shown in Table 7.

3) Determining deterioration conditions of base-plate solder

According to the data in Table 5 and Table 6, the value of T_{LL} and T_{RR} can be calculated and listed in Table 8.

TABLE 7. Comparison of steady state case temperature by using the actual measurement and BP neural network at different currents.

Case temperature different	Currents		
	30 A	50 A	75 A
T_{BML}	2.3°C	4.4°C	5.1°C
T_{ML}	3.9°C	7.3°C	8.8°C
T_{BMR}	2.7°C	5.0°C	6.6°C
T_{MR}	4.5°C	12.2°C	17.3°C

TABLE 8. Comparison of results about two simulations.

Result	Currents		
	30 A	50 A	75 A
T_{LL}	2.1°C	5.9°C	8.7°C
T_{RR}	1.9°C	1.6°C	1.7°C
Deteriorated side	Left side	Left side	Left side

TABLE 9. Deterioration degrees at different currents.

Deterioration degrees	Currents		
	30 A	50 A	75 A
g(T_{ML})	0.6957	0.6591	0.7255

Due to the result of $T_{LL} > T_{RR}$, the left side base-plate solder of IGBT module is more deteriorated than the right side.

4) Results of deterioration degrees

According to the calculation flowchart of degradation degree in Figure 10, based on the data in Table 5 and Table 7 the assessment results of base-plate solder are calculated and shown in Table 9. Under different excitation currents, the results are slightly different, and the range of deterioration degree is 0.6591∼0.7255. According to regulation of deterioration degree grade in section III.A, the assessment rank of base-plate solder should be "Alert". In addition, according to the reference [11], when the desquamating degree is greater than 50%, the power module failure probability is larger. Hence, when the desquamating degree is 17%, it is reasonable that the assessment rank of base-plate solder is "Alert".

VI. CONCLUSIONS

In this paper, an IGBT module of wind turbine converter is taken as the research object, and a health condition assessment method of base-plate solder fatigue for IGBT module based on case temperature difference is proposed. The major conclusions after analyzing results is given as follows: 1) With the increase of desquamating degree, the junction and case temperature of all IGBT chips rise. Compared with the junction and case temperature on both sides of IGBT chip, the middle chip temperature is highest. 2) By comparing the monitored and simulated data, the 3D finite element model is validated. Besides, the finite element simulation data are used as the training samples for the BP neural network, and the simulation data of case temperature can meet the

requirement of proposed assessment model. 3) The case temperature difference as the characteristic quantity can be used to reflect the base-plate solder health condition of multi-chip IGBT module. Using the proposed assessment method, the deterioration degree of base-plate solder for multi-chip IGBT module can be obtained effectively. Furthermore, the proposed assessment method could be used to the condition monitoring and control of wind turbine for the health management, which is helpful in improving operation and maintenance strategies which further to increase the operational reliability for wind turbines.

REFERENCES

[1] X. Du *et al.*, "Effect of wind speed probability distribution on lifetime of power semiconductors in the wind power converters," *Trans. China Electrotech. Soc.*, vol. 30, no. 15, pp. 109–117, 2015.
[2] U.-M. Choi, K. Ma, and F. Blaabjerg, "Validation of lifetime prediction of IGBT modules based on linear damage accumulation by means of superimposed power cycling tests," *IEEE Trans. Ind. Electron.*, vol. 65, no. 4, pp. 3520–3529, Apr. 2018.
[3] O. Noureldeen and I. Hamdan, "A novel controllable crowbar based on fault type protection technique for DFIG wind energy conversion system using adaptive neuro-fuzzy inference system," *Protection Control Mod. Power Syst.*, vol. 3, no. 3, pp. 328–339, 2018.
[4] F. Spinato, P. J. Tavner, G. J. W. van Bussel, and E. Koutoulakos, "Reliability of wind turbine subassemblies," *IET Renew. Power Generat.*, vol. 3, no. 4, pp. 387–401, Dec. 2009.
[5] Z. Chu *et al.*, "Fault diagnosis system of wind power converter based on wavelet neural network," *Electr. Eng.*, no. 9, pp. 34–37, 2012.
[6] W. Lai *et al.*, "IGBT lifetime model based on aging experiment," *Trans. China Electrotech. Soc.*, vol. 31, no. 24, pp. 173–180, 2016.
[7] H. Li, S. Liu, and L. Ran, "Overview of condition monitoring technologies of power converter for high power grid-connected wind turbine generator system," *Trans. China Electrotech. Soc.*, vol. 31, no. 8, pp. 1–10, 2016.
[8] K. B. Pedersen and K. Pedersen, "Dynamic modeling method of electro-thermo-mechanical degradation in IGBT modules," *IEEE Trans. Power Electron.*, vol. 31, no. 2, pp. 975–986, Feb. 2016.
[9] Y. Tian, X. Zhang, X. Xie, S. She, C. Lü, and R. Wang, "Thermal fatigue effects on IGBT die attach reliability," *Res. Prog. Solid State Electron.*, vol. 34, no. 3, pp. 288–292, 2014.
[10] P. Z. He, L. B. Zheng, H. C. Fang, C. L. Wang, and J. Hua, "Investigation of the temperature character of IGBT failure mode based the 3-D thermal-electro coupling FEM," *Adv. Mater. Res.*, vols. 655–657, no. 7, pp. 1576–1580, 2013.
[11] T. Lhommeaua, C. Martin, M. Karama, R. Meuret, and M. Mermet-Guyennet, "Base-plate solder reliability study of IGBT modules for aeronautical application," in *Proc. EPE*, Sep. 2007, pp. 1–10.
[12] B. Gao, F. Yang, M. Chen, L. Ran, I. Ullah, S. Xu, and P. Mawby, "A temperature gradient-based potential defects identification method for IGBT module," *IEEE Trans. Power Electron.*, vol. 32, no. 3, pp. 2227–2242, Mar. 2017.
[13] H. Li, Y. Hu, S. Liu, Y. Li, X. Liao, and Z. Liu, "An improved thermal network model of the IGBT module for wind power converters considering the effects of base-plate solder fatigue," *IEEE Trans. Device Mater. Rel.*, vol. 16, no. 4, pp. 570–575, Dec. 2016.
[14] A. S. Bahman, K. Ma, and F. Blaabjerg, "A lumped thermal model including thermal coupling and thermal boundary conditions for high-power IGBT modules," *IEEE Trans. Power Electron.*, vol. 33, no. 3, pp. 2518–2530, Mar. 2018.
[15] D. Xiang, L. Ran, P. Tavner, A. Bryant, S. Yang, and P. Mawby, "Monitoring solder fatigue in a power module using case-above-ambient temperature rise," *IEEE Trans. Ind. Appl.*, vol. 47, no. 6, pp. 2578–2591, Nov./Dec. 2011.
[16] M. Chen *et al.*, "Lifetime evaluation of IGBT module considering 513 fatigue accumulation of solder layers," *Proc. CSEE*, vol. 38, no. 20, pp. 6053–6061, 2018.
[17] H. Li, S. Liu, Y. Li, D. Yang, Y. Liang, and J. Liu, "Junction temperature evaluation model for IGBT module of wind-power converter considering multi-thermal coupling," *Electr. Power Autom. Equip.*, vol. 36, no. 2, pp. 51–56, 2016.
[18] S. Boubzizi, H. Abid, A. El Hajjaji, and M. Chaabane, "Comparative study of three types of controllers for DFIG in wind energy conversion system," *Protection Control Mod. Power Syst.*, vol. 3, no. 1, p. 21, 2018.
[19] H. Li *et al.*, "Gradual deterioration probability analysis based on temperature characteristic parameters for critical components of wind turbine generator system," *Electr. Power Autom. Equip.*, vol. 35, no. 11, pp. 1–7, 2015.

YAOGANG HU received the B.S. degree in electrical engineering from Yanshan University, China, in 2008, and the M.S. and Ph.D. degrees in electrical engineering from Chongqing University, China, in 2011 and 2017, respectively. He was a Lecturer with the Chongqing University of Technology, Chongqing, China. His research interests include condition monitoring, fault diagnosis, lifetime prediction, and performance assessment for wind power convertor.

PINGPING SHI received the B.S. degree in electrical agriculture science from Huazhong Agricultural University, China, in 2009, and the M.S. and Ph.D. degrees in economics and business administration from Chongqing University, Chongqing, China, in 2013 and 2018, respectively. She was a Lecturer with the Chongqing University of Technology, Chongqing. Her research interests include power enterprise cooperation, open and ever-growing electricity market, and operations' strategy of power equipment.

HUI LI received the M.Eng. and Ph.D. degrees in electrical engineering from Chongqing University, Chongqing, China, in 2000 and 2004, respectively. He was a Postdoctoral Research Fellow with the Institute of Energy Technology, Aalborg University, Denmark, from 2005 to 2007. Since 2008, he has been a Professor with the Department of Electrical Machinery and Electrical Apparatus, School of Electrical Engineering, Chongqing University, where he is currently a Researcher with the State Key Laboratory of Equipment and System Safety of Power Transmission and Distribution & New Technology. His main research interests include wind power generation, and design and control of electrical machines.

CHAO YANG received the Ph.D. degree in electrical engineering from Chongqing University, Chongqing, China, in 2015. He was a Senior Engineer with State Grid, Qinhuangdao Electric Power Supply Company, Qinhuangdao, China, from 2015 to 2018. In 2018, he joined the Chongqing University of Technology, Chongqing, China, as a Lecturer. His research interest includes renewable power generation and its grid connections.